Progress In Electromagnetics Research Letters, Vol. 90, 61–67, 2020

Towards Embedded RadCom-Sensors in Wind Turbine Blades: Preliminary Numerical and Experimental Studies

Jonas Simon[1], Jochen Moll[1, *], Viktor Krozer[1], Thomas Kurin[2], Fabian Lurz[2], Robert Weigel[2], Stefan Krause[3], Oliver Bagemiel[3], Andreas Nuber[4], and Vadim Issakov[5]

Abstract—This paper presents a numerical study on the application of radar and communication (RadCom) sensor nodes operating in the frequency band from 57–64 GHz. The sensor nodes are embedded in the laminate of wind turbine blades, enable a quality inspection directly after rotor blade manufacturing as well as a structural health monitoring (SHM) throughout the service life of the blade. Given by a lack of dielectric properties for typical rotor blade materials, we have performed experimental studies on material characterization including glass fibre composites, balsa wood, infusion glue, etc. This material database serves as input for wave propagation simulations in a full scale 3D rotor blade model. The analysis also includes a parametric study on path losses as well as an optimal sensor placement strategy.

1. INTRODUCTION

Rotor blades are a critical component of wind turbine structures, and detecting material failures is a nontrivial task given by their large dimensions of many tens of metres. A recent review shows the latest developments in the field of microwave, mm-wave, and THz testing of glass fibre composites [1]. Several sensing concepts are available such as transmission line methods, open-ended probe methods, free space measurements, and resonance-based methods. Some of those approaches are permanently used in a structural health monitoring (SHM) framework. An example is a dual-band radar system (24 GHz and 35 GHz) proposed in [2, 3] for SHM of wind turbine blades. In those works, the FMCW radar was fixed to the tower of a wind turbine and radiated electromagnetic waves towards the rotor blades. Inspection was performed when the blades passed the radar sensor. Doppler radar systems can also be used for SHM purposes measuring the mechanical vibrations of the wind turbine [4]. Moreover, guided electromagnetic waves can be used for surface damage detection of structural components [5, 6].

A key aspect of every SHM system is given by the fact that sensors must be permanently attached to the structure so that baseline measurements can be recorded during a training phase [7]. Relative signal changes recorded in a monitoring phase can be regarded as structural damage. In this work, we propose an autonomous RadCom sensor node network for SHM purposes, which is embedded in the wind turbine blade during manufacturing. It combines radar and communication functionalities as suggested in the Radar 2020 concept [8] and in [9, 10]. By means of this sensor, two aspects are covered at the same time: on the one hand, the rotor blade quality after production can be evaluated with a high degree of automation; on the other hand, structural monitoring of the rotor blades can be achieved

Received 10 December 2019, Accepted 31 January 2020, Scheduled 9 March 2020

* Corresponding author: Jochen Moll (moll@physik.uni-frankfurt.de).

[1] Department of Physics, Goethe University of Frankfurt, Max-von-Laue-Str. 1, Frankfurt/Main 60438, Germany. [2] Friedrich-Alexander University Erlangen-Nuremberg, Institute for Electronics Engineering, Erlangen 91058, Germany. [3] Fraunhofer Institute for Wind Energy and Energy System Technology, Bremerhaven 27572, Germany. [4] Wölfel Engingeering GmbH + Co. KG, Höchberg 97204, Germany. [5] Infineon Technologies AG, Neubiberg 85579, Germany.

during ongoing wind turbine operation. Wireless communication for data exchange between adjacent sensor nodes eliminates the need for long cable runs in the rotor blade.

In this paper, we perform wave propagation analysis for embedding RadCom sensor nodes in rotor blade laminates. Given by experimentally determined material parameters of typical rotor blade materials an optimal sensor placement strategy is carried out. The paper is organized as follows. Section 2 presents the numerical modelling strategy followed by the material characterization in Section 3. Finally, results are presented and discussed in Section 4.

2. NUMERICAL ROTOR BLADE MODEL

In the following, we assume a rotor blade of 41 m length depicted in Fig. 1. It can be regarded as a large heterogeneous dielectric medium. The simulation covers a frequency range from 57 to 64 GHz while multiple scattering effects are neglected. This leads to a model of the received signal in the frequency domain that is given by

$$Y(r,\omega) = U(\omega)P(r,\omega) + N(\omega), \tag{1}$$

where r is the distance with $r = 0$ at the transmitter position and ω the angular frequency. $U(\omega)$ denotes the spectrum of the transmitted signal and $N(\omega)$ the spectrum of the superimposed normally distributed measurement noise. $P(r,\omega)$ represents the phase-term that models the propagation through the heterogeneous dispersive medium and is given by

$$P(r,\omega) = \sum_{n=1}^{N_S} \exp\left(i\,\underline{k}_n(\omega)\,r_n\right). \tag{2}$$

This expression assumes that the heterogeneous medium consists of $n = 1 \ldots N_S$ sections in which the wave travels a distance r_n. Each region can have a different frequency-dependent complex wavenumber $\underline{k}_n(\omega)$ which is defined as $\underline{k}_n(\omega) = k_0 \cdot \sqrt{\underline{\varepsilon}_n(r,\omega)}$. Here, k_0 denotes the vacuum wavenumber and $\underline{\varepsilon}_n(r,\omega)$ the complex and frequency-dependent permittivity of the n-th dielectric region. For simplicity, an orthogonal incidence is assumed here for modelling the transmission and reflection properties.

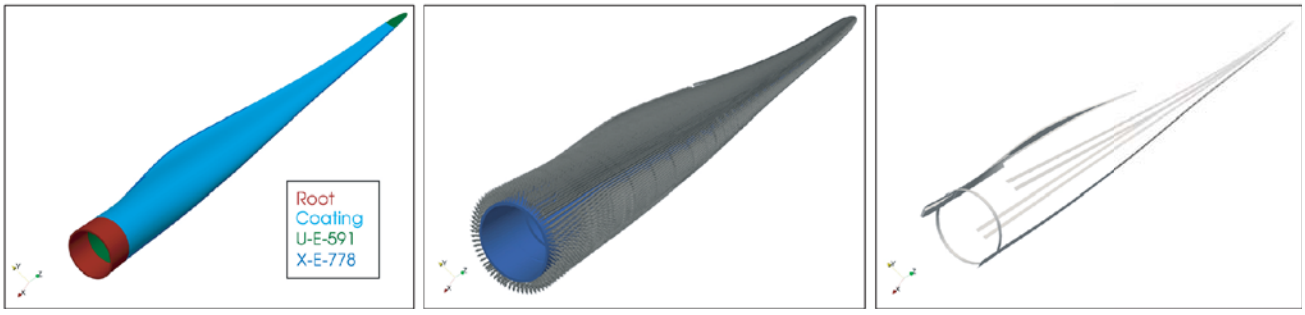

(a) (b) (c)

Figure 1. (a) Rotor blade model visualized in ParaView where each material has a different color (see also Table 1). (b) Surface normals (c) Segmented view with only one material. The blade has a total length of 41 m and a diameter at the blade root of 1.9 m.

3. MATERIAL CHARACTERIZATION

To derive the complex permittivity of the rotor blade materials a free space setup is used [11]. To extract unambiguous results the materials are measured with two different thicknesses, as the used method of minimizing the difference between the measured signal and theoretical calculated values would create multiple ambiguous results [12].

3.1. Experimental Setup

To create a suitable measurement setup, two horn antennas are placed opposite to each other with the material in-between. With a microwave network analyzer a frequency sweep in the range from 55 GHz to 65 GHz is performed, and the signal transmitted through the material is measured. To allow for tolerances in the material alignment, the sample is rotated throughout the measurement. The lowest calculated value for ε_r corresponds to an orthogonal wave incident and therefore to the correct value. To prevent the signal from passing around the materials, they are placed in a PVC-frame with attached absorbing material as can be seen in Fig. 2. The frame allows mounting of different materials within the thickness range of 5 mm to 20 mm.

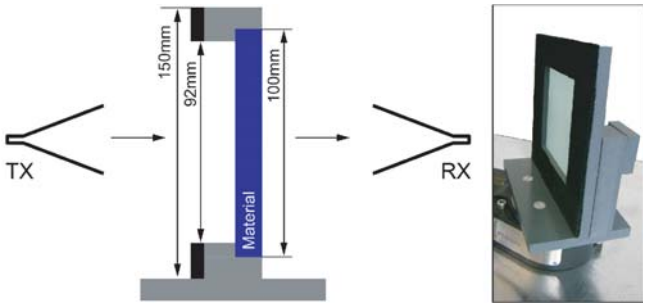

Figure 2. Measurement setup for free space material characterization using a PVC (Polyvinylchloride) sample-mount with nylon screws covered by absorbent foam with an effective opening of 92×92 mm.

3.2. Characterization

The measured transmission values are time domain gated to remove artifacts caused by multiple reflections. Then using the dual thickness algorithm described in [13] the permittivity is extracted for each rotation step of the material, and the minimal value is saved. As some of the rotor blade materials could not be produced in multiple thicknesses, an unambiguous calculation of the permittivity is not possible. For this reason, only one of the ambiguous solutions is physically meaningful. The calculated values are listed in Table 1.

Table 1. Measured ε_r and $\tan\delta$ of rotor blade materials in the frequency band from 55 GHz to 65 GHz.

Material	ε_r	$\tan\delta$
Balsa wood BALTEK SB100	1.197	0.0586
EPIKOTE resin	2.902	0.0260
Infusion glue	3.059	0.0293
Saertex U-E-591 g/m^2	4.545	0.0399
Saertex X-E-778 g/m^2	4.709	0.0291
Saertex U-E-1182 g/m^2	4.962	0.0305
Saertex K-E-1175 g/m^2	5.307	0.0329

4. RESULTS

The following section describes the results of the numerical analysis of the full rotor blade model using the material parameters from the previous section. First, results of parametric studies are presented including the analysis of dielectric losses. After that, a possible sensor placement strategy is proposed.

4.1. Parametric Studies

RadCom-sensors should be embedded in the laminate close to the outer layer of the rotor blade so that external power supply can be realized by solar foils that are installed on the surface of the blades. This potentially leads to two possible inspection scenarios. In the first case, wave propagation and inspection can be realized in the hull of the blade. It means that high dielectric losses could be expected from the glass fibre reinforced plastic (GFRP) material, see Table 1. In the second case, the inspection takes place on the opposite side of the rotor blade. In this case, the electromagnetic waves propagate largely in air, and only a small propagation distance is in the GFRP composite.

Figure 3 depicts the dielectric losses for the first scenario when the wave propagation is in the hull of the rotor blade. Based on the dielectric properties of K-E-1175 g/m^2 it can be seen that a relatively small sensing radius of 10 cm can be achieved assuming a signal attenuation of −40 dB. Based on this observation, we have considered the second scenario in Fig. 4, where the dielectric losses in radial direction are presented. In this representation, a cross-section of the blade has been considered

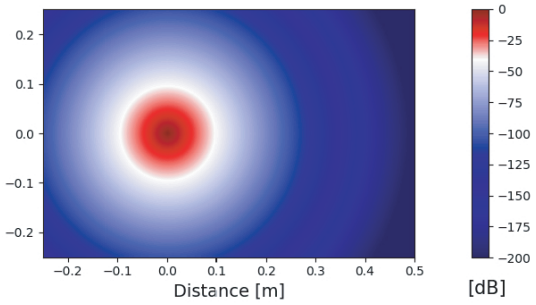

Figure 3. Simulated wave propagation in the hull of the rotor blade using the dielectric properties of K-E 1175 g/m^2 (glass fibre composite). The dielectric losses are relatively high so that a limited area could be inspected inside the hull. The −40 dB region is color-coded by a white circle.

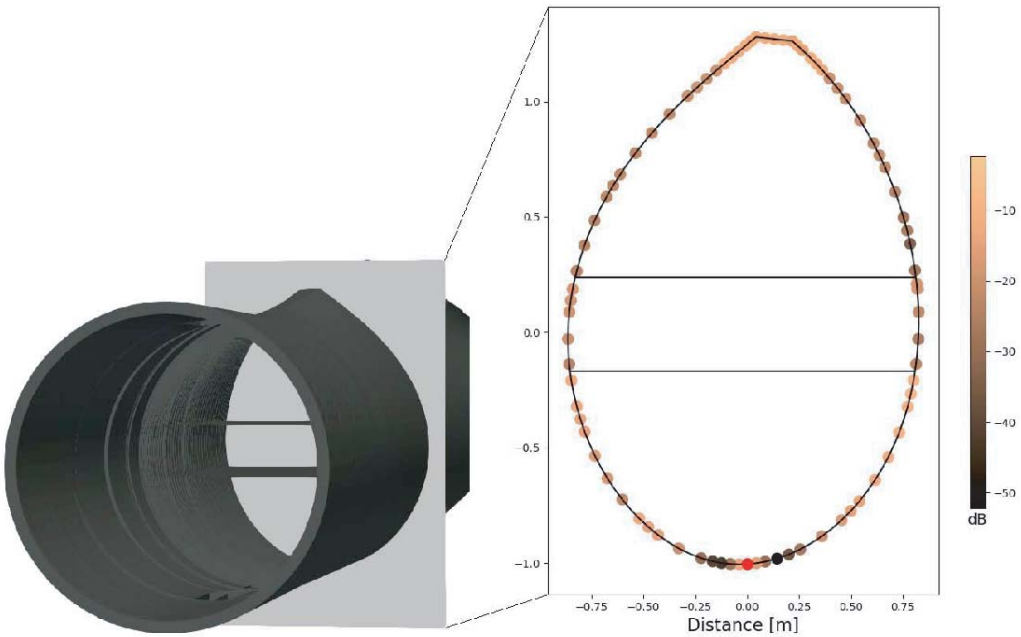

Figure 4. Radial losses are small so that a monitoring of the opposite side is a possible solution for structural monitoring. The transmitter is highlighted at the bottom of the figure by a red dot.

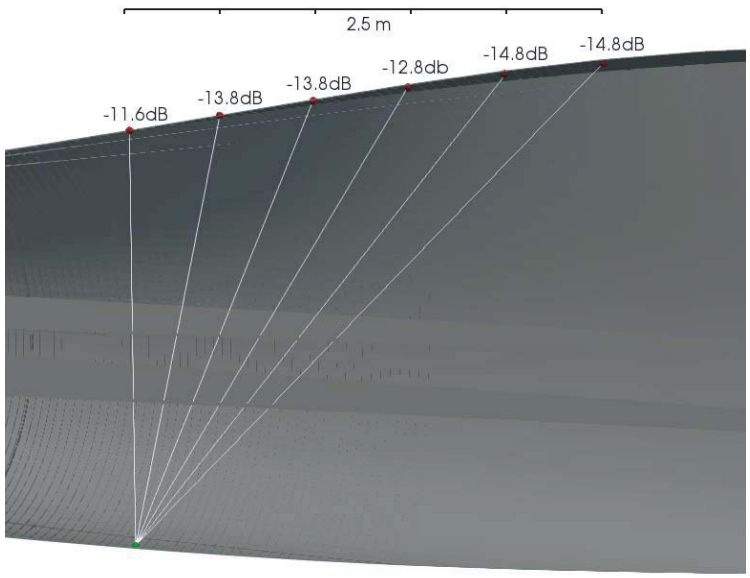

Figure 5. Dielectric losses on the round-trip path from the sensor node to the top surface of the hull on the opposite side of the blade and back. The losses are depicted for different radial directions.

next to the blade root which is the worst case scenario. It can be observed that the losses are relatively small so that this approach could be a feasible solution for the proposed SHM system. Finally, we have considered the dielectric losses in different directions inside the blade model as shown in Fig. 5. The losses are moderate so that a hybrid radar inspection and communication methodology along the axial direction of the blade seems possible.

4.2. Sensor Placement Strategy

Since a full field electromagnetic simulation is not possible for optimal placement of RadCom-sensor nodes, we have performed a simplified numerical analysis using the framework described before. The sensor placement strategy assumes an antenna opening angle of $\pm 30^\circ$ perpendicular to the surface that illuminates the opposite side of the blade. Dielectric loading of the antenna has been neglected. Additional sensor nodes are placed along the blade in such a way that each point of the blade is covered by at least two adjacent RadCom sensor nodes (except directly at the blade root). On the one hand, this approach improves reliability in case of a sensor node failure. On the other hand, a localization of structural damage can be achieved by triangulation and digital beamforming techniques [14]. Fig. 6 shows a possible structure of the sensor arrangement. This optimization approach leads to the case that the sensor density at large blade cross-sections is smaller than regions next to the blade tip.

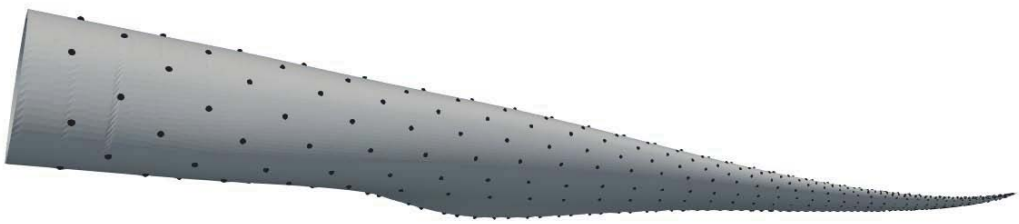

Figure 6. Sensor placement strategy for a 41 m long rotor blade assuming that each point of the rotor blade is covered by at least two adjacent RadCom sensor nodes (except directly at the blade root).

5. CONCLUSIONS

The work presented in this paper aimed at a structural health monitoring approach in which RadCom-sensor nodes in the frequency band from 57–64 GHz were embedded in the laminate of wind turbine blades. Besides experimental characterization of typical rotor blade materials, we have performed a numerical study on dielectric path losses and optimal sensor placement. Future research will focus on the realization of RadCom sensor nodes and their embedding in the laminate. Moreover, we will perform experimental fatigue tests to evaluate the radar-based detection performance for various typical material defects such as inter-fibre failure, delamination, fiber ondulation, and bondline cracks.

ACKNOWLEDGMENT

The authors gratefully acknowledges the financial support of this research by the Federal Ministry for Economic Affairs and Energy (Grant Number: 0324324C).

REFERENCES

1. Li, Z., A. Haigh, C. Soutis, A. Gibson, and P. Wang, "A review of microwave testing of glass fibre-reinforced polymer composites," *Nondestructive Testing and Evaluation*, 1–30, April 2019.
2. Moll, J., J. Simon, M. Mälzer, V. Krozer, D. Pozdniakov, R. Salman, M. Dürr, M. Feulner, A. Nuber, and H. Friedmann, "Radar imaging system for in-service wind turbine blades inspections: Initial results from a field installation at a 2 MW wind turbine," *Progress in Electromagnetic Research*, Vol. 162, 51–60, 2018.
3. Moll, J., P. Arnold, M. Mälzer, V. Krozer, D. Pozdniakov, R. Salman, S. Rediske, M. Scholz, H. Friedmann, and A. Nuber, "Radar-based structural health monitoring of wind turbine blades: The case of damage detection," *Structural Health Monitoring*, Vol. 17, No. 4, 815–822, July 2018.
4. Ochieng, F. X., C. M. Hancock, G. W. Roberts, and J. Le Kernec, "A review of ground-based radar as a noncontact sensor for structural health monitoring of in-field wind turbines blades," *Wind Energy*, July 2018.
5. Moll, J., "Damage detection and localization in metallic structures based on jointed electromagnetic waveguides: A proof-of-principle study," *Journal of Nondestructive Evaluation*, Vol. 37, No. 4, December 2018.
6. Moll, J., "Numerical and experimental analysis of defect detection in jointed electromagnetic waveguides," *13th European Conference on Antennas and Propagation*, 1–4, 2019.
7. Worden, K., C. R. Farrar, G. Manson, and G. Park, "The fundamental axioms of structural health monitoring," *Proceedings of the Royal Society A: Mathematical, Physical and Engineering Sciences*, Vol. 463, No. 2082, 1639–1664, June 2007.
8. Wiesbeck, W. and L. Sit, "Radar 2020: The future of radar systems," *2014 International Radar Conference (Radar)*, 1–6, October 2014.
9. Ciuonzo, D., A. De Maio, G. Foglia, and M. Piezzo, "Intrapulse radarembedded communications via multiobjective optimization," *IEEE Transactions on Aerospace and Electronic Systems*, Vol. 51, No. 4, 2960–2974, October 2015.
10. Ciuonzo, D., A. De Maio, G. Foglia, and M. Piezzo, "Pareto-theory for enabling covert intrapulse radar-embedded communications," *2015 IEEE Radar Conference (RadarCon)*, 0292–0297, Arlington, VA, USA, May 2015.
11. Brancaccio, A., G. D'Alterio, E. De Stefano, L. Di Guida, M. Feo, and S. Luce, "A free-space method for microwave characterization of materials in aerospace application," *2014 IEEE Metrology for Aerospace (MetroAeroSpace)*, 423–427, May 2014.
12. Arslanagić, S., T. V. Hansen, N. A. Mortensen, A. H. Gregersen, O. Sigmund, R. W. Ziolkowski, and O. Breinbjerg, "A review of the scattering-parameter extraction method with clarification of ambiguity issues in relation to metamaterial homogenization," *IEEE Antennas and Propagation Magazine*, Vol. 55, No. 2, 91–106, April 2013.

13. Lau, I., M. Frank, K. Shi, F. Lurz, A. Talai, R. Weigel, and A. Koelpin, "An accurate free space method for material characterization in w- band using material samples with two different thicknesses," *2018 48th European Microwave Conference (EuMC)*, 202–205, September 2018.
14. Moll, J., T. N. Kelly, D. Byrne, M. Sarafianou, V. Krozer, and I. Craddock, "Microwave radar imaging of heterogeneous breast tissue integrating A-priori information," *International Journal of Biomedical Imaging*, Article ID 943549, 10, 2014.